Plasma Processing Approach to Molecular Surface Tailoring of Nanoparticles: Improved Photocatalytic Activity of TiO_2

Jai Cho,[†] Ferencz S. Denes,[‡] and Richard B. Timmons*,[†]

Environmental Sciences and Engineering Program, Department of Chemistry and Biochemistry, University of Texas at Arlington, Arlington, Texas 76019, and Department of Biological Systems Engineering and Center for Plasma Aided Manufacturing, University of Wisconsin, Madison, Wisconsin 53706

Received January 26, 2006. Revised Manuscript Received April 5, 2006

Plasma enhanced chemical vapor deposition (PECVD) was employed to modify surfaces of TiO_2 nanoparticles. To help overcome nanoparticle aggregation, a 360° rotating reactor was employed to provide continuous agitation and mixing of the particles during the plasma induced film deposition process. The nanoparticles were coated with thin films produced from the plasma polymerization of tetramethyltin (TMT) monomer. Subsequently, the coated particles were heated in air to remove the carbonaceous material while, simultaneously, oxidizing the tin atoms to tin oxide. The photocatalytic activity of the tin oxide coated TiO_2 was then measured and contrasted with that of untreated TiO_2 particles. A significantly enhanced increase in the oxidation rate of acid orange (AO7) dye was observed with the modified particles. Additional experiments employing a mixture of TMT and perfluoropropylene oxide monomers were used to achieve surfaces possessing partially fluorinated tin oxide. The fluorine doped tin oxide coatings exhibited even higher catalytic activity than that obtained from TMT only experiments. Some experiments involving characterization of the films before and after the annealing process, specifically those involving X-ray diffraction and atomic force microscopy measurements, were carried our using flat glass or polished silicon substrates. Overall, this study demonstrates the general utility of PECVD technology to provide effective coating of ultrafine nanoscale particles.

Introduction

Improvement of the photocatalytic activity of TiO_2 has been the subject of numerous studies in recent years. In large part, these studies reflect the many potential uses of TiO_2 in applications such as environmental remediation, nonfouling surfaces, and energy conservation and conversion processes. Much of this interest arises from the many favorable attributes of this compound which include relatively low cost and nontoxicity along with the fact that sunlight may be employed for the photoactivation process. It is now well-established that photoactivation induces formation of electron−hole pairs in the conduction and valence bands. The potential energy of the photogenerated electrons and holes can be transferred to a redox couple with appropriate redox potential, that is, less positive than that of the valence band and less negative than that of the conduction band of the semiconductor. As a result, the TiO_2 can be employed for both photocatalytic oxidation and reduction reactions, dependent on reaction conditions.

Unfortunately, rapid recombination of such charge carriers is often found to be a major limiting factor that controls the efficiency of the photocatalysts.[1−5] Numerous methods have been employed to retard such recombination including the addition of surface dopants,[6,7] electron or hole scavengers adsorbed on the surface,[8,9] and more recently, development of coupled semiconductors.[10−14] Coupling of two semiconductors, having different redox energy levels for their corresponding conduction and valence bands, provides an attractive approach to more efficient charge separation. Efficient charge separation increases the lifetime of the charge carriers and improves the efficiency of the interfacial charge transport to the adsorbed target substrates. For example, it was reported that the photogenerated electrons from CdS can be injected into the TiO_2 conduction band while photoinduced holes remain on CdS.[15−17] This interparticle electron transfer (IPET) pathway affords irreversible "vectorial electron transfer", for which a rate of 5×10^{10}/s

* To whom correspondence should be addressed. E-mail: timmons@uta.edu.
[†] University of Texas at Arlington.
[‡] University of Wisconsin.

(1) Serpone, N.; Maruthamuthu, P.; Pichat, P.; Pelizzetti, E.; Hidaka, H. *J. Photochem. Photobiol.* **1995**, *85*, 247.
(2) Tada, H.; Hattori, A.; Tokihisa, Y.; Imai, K.; Tohge, N.; Ito, S. *J. Phys. Chem. B* **2000**, *104*, 4585.
(3) Kumar, A.; Jain, A. K. *J. Mol. Catal.* **2001**, *165*, 265.
(4) Yin, H.; Wada, Y.; Kitamura, T.; Sakata, T.; Mori, H.; Yanagida, S. *Chem. Lett.* **2001**, *4*, 334.
(5) Hirai, T.; Suzuki, K.; Komasawa, I. *J. Colloid Interface Sci.* **2001**, *244*, 262.
(6) Choi, W.; Hoffmann, M. R. *J. Phys. Chem.* **1995**, *98*, 13669.
(7) Esposito, G.; Zanobi, A.; Giglio, E.; Pavel, N. V.; Campbell, I. D. *J. Phys. Chem.* **1995**, *91*, 83.
(8) Kamat, P. V.; Dimitrijevic, N.; Fessenden, R. W. *J. Phys. Chem.* **1988**, *92*, 2324.
(9) Kamat, P. V.; Dimitrijevic, N. *J. Phys. Chem.* **1989**, *93*, 4259.
(10) Bessekhouad, Y.; Robert, D.; Weber, J. V. *J. Mol. Catal. A* **2004**, *223*, 161.
(11) Tatsuma, T.; Saitoh, S.; Ngaotrakanwiwat, P.; Ohko, Y.; Fujishima, A. *Langmuir* **2002**, *18*, 7777.
(12) Wu, C. *Chemosphere* **2004**, *57*, 601.
(13) Okada, M.; Yamada, Y.; Jin, P.; Tazawa, M.; Yoshimura, K. *Thin Solid Films* **2003**, *442*, 217.
(14) Subasri, R.; Shinohara, T. *Electrochem. Commun.* **2003**, *5*, 897.
(15) Redmond, G.; O'Keeffe, A.; Burgess, C.; MacHale, C.; Fitzmaurice, D. *J. Phys. Chem.* **1993**, *97*, 11081.

10.1021/cm060212g CCC: $33.50
Published on Web 05/16/2006

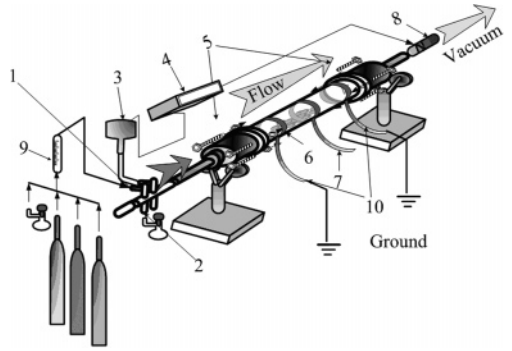

Figure 1. Schematic diagram of the 360° rotating RF plasma reactor. 1, gas inlet port; 2, secondary gas inlet port (for low vapor pressure reaction precursor); 3, MKS Baratron pressure transducer; 4, exhaust valve controller; 5, ferrofluidic feed-through valves inside aluminum housing; 6, ground electrode; 7, hot electrode; 8, butterfly valve; 9, flowmeter; and 10, two external ground electrodes.

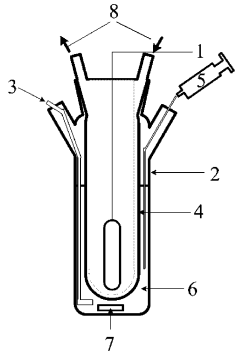

Figure 2. Schematic diagram of the photochemical reactor. 1, UV light source; 2, reactor vessel; 3, sparging gas flow; 4, immersion well; 5, sample withdrawing port; 6, TiO_2 and substrates aqueous suspension; 7, magnetic stirring bar; 8, cooling water flowing in and out through the jacket inside of the immersion well.

was reported in CdS/TiO_2 or ZnO colloidal systems under certain conditions.[18] In addition, simultaneous charge carrier transfer, that is, electrons from CdS to TiO_2 and holes from TiO_2 to CdS, was reported to develop efficient charge separation in aqueous bi-semiconductor dispersion systems.[19,20]

In the present study we report, for this first time, a hybrid TiO_2 plus second semiconductor composite fabricated via a plasma processing technique, specifically plasma enhanced chemical vapor deposition (PECVD). In contrast with the coupled semiconductors noted above, which involved basically simple physical mixtures of the two different particles, the plasma processing approach involves synthesis of a composite particle in which the second compound, in this case SnO_2, is solidly grafted to the core TiO_2 particles. Subsequently, the photocatalytic activities of the composite particles were compared with the unmodified TiO_2, as measured using the photo-oxidation of an organic dye. As documented below, a substantial increase in catalytic activity, as high as 80%, was observed with the plasma synthesized composite particles.

Experimental Methods

Preparation of the Hybrid Catalyst. As a precursor of the semiconductor oxide film, tin-containing organometallic thin films were deposited on the surface of TiO_2 particles via radio frequency (RF) plasma polymerization. The TiO_2 particles employed were the Degussa P-25 standard (80% anatase, 20% rutile) having a number average particle diameter of 21 nm. In an effort to achieve efficient coating of the TiO_2 nanoparticles, a 360° continuously rotatable plasma reactor, as depicted in Figure 1, was constructed for this purpose. The dimensions of the cylindrical reactor were 5 cm i.d. and 46 cm in length. Obtaining the rotational motion while maintaining vacuum was achieved via use of Ferrofluidic valves located at each end of the reactor, as identified in Figure 1.[21] Transport grooves, located on the inside of the glass reactor, move the particles upward during rotation for subsequent gravitational descent through the plasma discharge. It is believed that this efficient mass transport and agitation of the particles provide continuous exposure of the fresh surface of the TiO_2 particles to the plasma generated reactive molecules and ions. This is an important consideration because the nanoscale TiO_2 particles employed are prone to aggregation. In a typical run, 3.5 g of TiO_2 particles were loaded inside the borosilicate glass reactor, and the reactor was evacuated to 8 mTorr background pressure. After the background pressure was reached, an oxygen plasma pretreatment was conducted at 100 W average power to remove any carbonaceous contaminants on the surface of TiO_2 particles. Subsequently, the PECVD process was initiated using tetramethyltin (TMT, Aldrich) monomer. In some experiments, hexafluoropropylene oxide (C_3F_6O, Aldrich) was added to the TMT monomer vapor, as described later in this paper. After plasma deposition of the tin-containing films on the TiO_2 particles, thermal treatments were carried out on these composite materials at temperatures ranging 300−600 °C. The high-temperature annealing processes were conducted in air to oxidize the tin to the oxide and, simultaneously, reduce the carbon content present on the particle surfaces.

Photocatalytic Oxidation of Azo-Containing Organic Dye. Acid orange 7 (AO7 or Orange II, Aldrich) was employed as the substrate to measure the photo-oxidation catalytic activities of both the modified and the unmodified TiO_2 particles. The AO7, a toxic waste product from the textile industry,[22] has been employed for this purpose in a number of previous studies of TiO_2 photocatalytic activity. In the present study, 500 mL aqueous solutions, containing a 500 μM concentration of AO7, were employed. Three hundred milligram samples of untreated or plasma treated TiO_2 particles were dispersed in the analyte solution contained in the photochemical reactor system, shown in Figure 2. The TiO_2-containing suspensions were strongly agitated and remained dispersed in the liquid by the flow of the oxygen sparging gas and by continuous magnetic stirring of the mixture throughout the course of the photolytic reactions. The TiO_2 plus analyte solutions were allowed to mix in the dark for 30 min, with constant stirring to permit adsorption equilibrium of the analyte onto the particles to be established. At this point, the first 5 mL aliquot was withdrawn from the solution, and this analyte concentration represents the starting ($t = 0$) concentration. The photochemical reaction was then initiated by igniting the light source immediately after the first sample was taken. Aliquots were then periodically withdrawn as the photo-oxidation reaction proceeded. Each aliquot was filtered

(16) Finlayson, M. F.; Wheeler, B. L.; Kakuta, N.; Park, K.; Bard, A. J.; Campion, A.; Fox, M. A.; Webber, S. E.; White, J. M. *J. Phys. Chem.* **1985**, *89*, 5676.
(17) White, J. R.; Bard, A. J. *J. Phys. Chem.* **1985**, *89*, 1947.
(18) Hotchandani, S.; Kamat, P. V. *J. Phys. Chem.* **1992**, *96*, 6834.
(19) Kamat, P. V. *Chem. Rev.* **1993**, *93*, 267.
(20) Serpone, N.; Borgarello, E.; Gratzel, M. *J. Chem. Soc., Chem. Commun.* **1984**, 342.
(21) Denes, F. *Trends Polym. Sci.* **1997**, *5*, 23.
(22) Boeninger, M. *Carcinogenicity and Metabolism of Azo Dyes Especially Those Derived From Benzidine*; DHHS (NIOSH) Publication 80-1 19; U.S. Government Printing Office: Washington, DC, July, 1990.

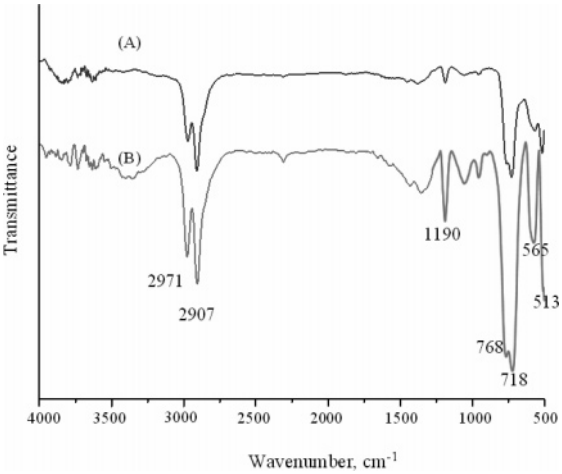

Figure 3. FT-IR transmission spectra of the pulsed plasma polymerized TMT thin films on KBr disks. (A) TMT film prepared with 10-ms-on/30-ms-off duty cycle; (B) TMT film prepared with 10-ms-on/200-ms-off duty cycle. Applied peak power was 150 W for both films.

through a 0.25 μm pore poly(vinylidene difluoride) syringe filter (Cobert Xpertek) to remove the catalyst particles. The absorbance of each filtered aliquot was then determined spectrophotometrically, using a UV−visible spectrometer (JASCO UV−vis 2350). The absorbance of each sample was measured at 484 nm, the wavelength maximum for AO7, and converted to concentrations using a Beer's law calibration curve for AO7. It was observed that direct photooxidation of the AO7 occurred to a small extent in the absence TiO_2. However, the direct rate was negligible to that observed under the photocatalytic conditions employed in this study.

Characterization of Plasma Deposited Tin-Containing Films. Preliminary experimental results revealed that the chemical compositions of the plasma generated films were independent of the substrates employed. That is, films deposited on flat substrates and particles were identical. Thus, to facilitate characterization of the films, many of the spectroscopic studies were carried out on TMT films deposited on polished silicon wafers under precisely identical plasma reactor conditions as those employed in coating the TiO_2 particles. The spectroscopic analyses included Fourier transform infrared (FT-IR), X-ray photoelectron spectroscopy (XPS), X-ray diffraction (XRD), atomic force microscopy (AFM), and transmission electron microscopy (TEM).

Results

On the basis of prior experiments with TMT,[23] plasma polymerization processes were conducted at a monomer pressure of 100 mTorr and a flow velocity of 0.5 cm^3/min (STP). Under these conditions, high quality, mechanically stable, tin-containing films are obtained. These prior studies revealed that TMT plasma polymer film compositional changes were observed with varying plasma duty cycles when polymerization was carried out under pulsed plasma conditions. IR spectra, shown in Figure 3, confirm this fact. In the present study, plasma duty cycle variation at 10-ms-on/30-ms-off and 10-ms-on/200-ms-off were examined. On the basis of the relative intensity of the CH stretching bands at 2971 and 2907 cm^{-1} compared to the tin-related bands between 850 and 500 cm^{-1}, it is clear that a relatively higher tin content was obtained under the lower duty cycle condition. A band at 565 cm^{-1}, attributed to Sn−O stretching modes, appears on the plasma polymerized TMT films despite the fact the TMT monomer does not contain any oxygen. However, the spontaneous oxidation of plasma films is not unusual, and it was observed in our prior study.[23] The presence of the Sn−O in plasma generated TMT films could arise from two sources. First, trace amounts of oxygen in the plasma reactor during polymerization might participate in the film formation process. Second, and more likely, the films are spontaneously oxidized by contact with the atmosphere after deposition.

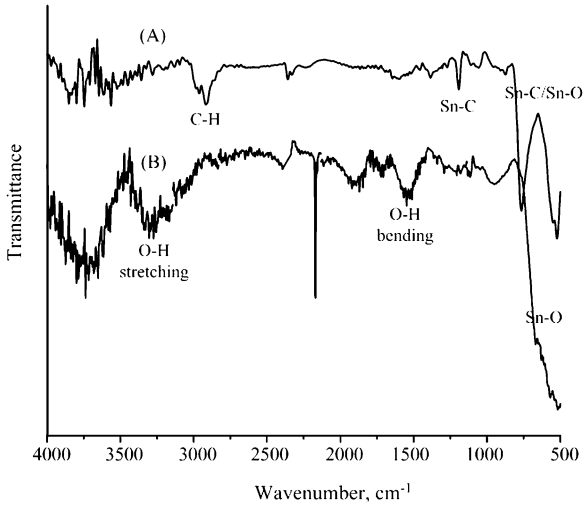

Figure 4. FT-IR transmission spectra of the plasma polymerized TMT thin films before and after thermal treatment. (A) TMT film prepared with 10-ms-on/30-ms-off duty cycle for 5 min, as-deposited; (B) the same film annealed at 425 °C for 5 h in air. Applied peak power was 150 W for both films deposited on KBr disks.

Figure 4 illustrates the IR spectral change of TMT plasma film after annealing, in air, at 425 °C for 5 h. The deposition of the original film on a KBr disk was carried out with a 10-ms-on/30-ms-off duty cycle at a 150 W peak power applied for 5 min. The resulting film was immediately transferred to the FT-IR instrument after deposition. After recording its IR spectrum, it was subjected to the high temperature heat treatment. Simultaneously, visual inspection of the films on silicon substrates confirmed that a film remained after the heat treatment. Several differences are apparent in contrasting the "as-deposited" and "thermally annealed" samples. One such difference is the absence of C−H stretching absorptions after thermal treatment, indicating that essentially complete thermal oxidation of hydrocarbon components took place. Additionally, it is clear that the IR absorptions in the lower wavelength regions by the "as-deposited" films were substantially changed by the heat treatment. The intense absorption which appears in the annealed sample, beginning at around 750 cm^{-1} and extending to the spectrometer cutoff wavelength, is interpreted to indicate formation of a Sn−O−Sn−O crystalline network rather than the amorphous Sn−O and/or Sn−C phase present in the as-deposited sample. Finally, one notes the appearance of broad absorption bands, centered at approximately 3300 and 1700 cm^{-1}, and a very sharp band at 2170 cm^{-1} in the annealed film. These absorptions are attributed to the presence of −OH stretching and bending motions and CO absorption on the high temperature annealed sample. In

(23) Chen, X. L.; Rajeshwar, K.; Timmons, R. B.; Chen, J. J.; Chyan, O. M. R. *Chem. Mater.* **1996**, *8*, 1067.

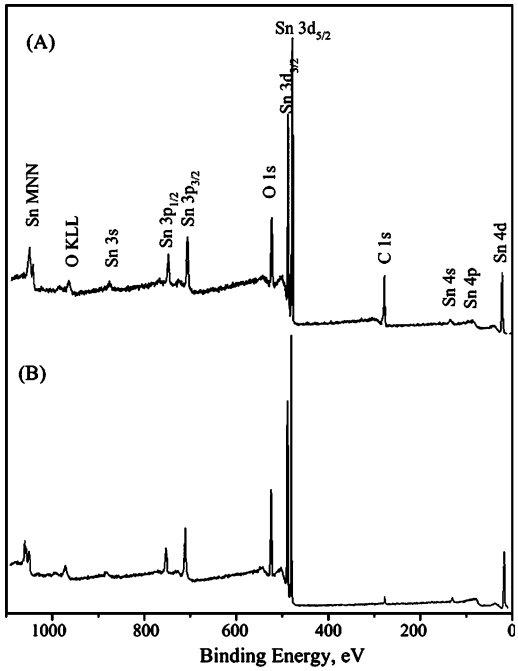

Figure 5. XPS survey scan spectra of the plasma polymerized TMT thin film deposited with different duty cycles after spontaneous oxidation at ambient exposure for 7 days. (A) 10-ms-on/30-ms-off; (B) 10-ms-on/200-ms-off after heat treatment for 5 h at 425 °C.

support of this assignment, it is noted that water contact angle measurements reveal that the film had become exceedingly hydrophilic as a result of the heat treatment. In fact, the water contact angle decreased from 80° to less than 5° (actually it was essentially nonmeasurable) which would be consistent with the presence of surface −OH groups being present. The sharp spike, at 2170 cm^{-1}, not present in the "as-deposited" film but prominent after the heat treatment, attributed to adsorbed CO, is in accord with prior studies that revealed strong CO adsorption on Sn^{4+} (2169 cm^{-1} [24]), Ti^{4+} (2173 cm^{-1},[25] 2179 cm^{-1}, and 2169 cm^{-1} [26,27]) and on Zr^{4+} (2170 cm^{-1} [28]). It is assumed that some CO is produced during the high temperature oxidation of the carbonaceous portion of the originally deposited TMT film.

XPS Analysis of TMT Plasma Films. Because the prior study[23] revealed that the initially deposited plasma TMT polymer films undergo rapid oxidation, all XPS analyses were conducted on the samples after exposure to ambient air for sufficient periods to permit completion of the spontaneous oxidation processes. XPS spectra clearly revealed that tin-containing polymeric films were successfully obtained by the pulsed plasma deposition process, with a slightly different tin content dependent on the duty cycle employed. A survey scan of the TMT film deposited using a plasma duty cycle of 10 ms on and 30 ms off is shown in Figure 5A. A slightly higher tin content was obtained using a lower duty cycle of 10 ms on and 200 ms off, as reported in Table 1.

Table 1. Relative Percent of Carbon, Oxygen, and Tin Present on the Surface of the Plasma Polymerized TMT Films before and after Thermal Treatment

sample	C(1s)	O(1s)	Sn($3d_{5/2}$)
TMT 10-ms-on/30-ms-off, no annealing	51.3%	29.4%	19.3%
TMT 10-ms-on/30-ms-off, annealed at 425 °C for 5 h	7.0%	63.9%	29.1%
TMT 10-ms-on/200-ms-off, no annealing	41.2%	33.1%	25.7%
TMT 10-ms-on/200-ms-off, annealed at 425 °C for 5 h	7.7%	63.5%	28.8%

Thermal treatment of these films induced significant compositional differences of the "as-deposited" materials, as depicted in Figure 5B. XPS spectra revealed that the annealing process transformed the as-deposited tin-containing organic films to essentially tin oxide films. For example, the atomic concentrations of carbon on the surface of the films, 51.3 and 41.2% for the higher and lower duty cycles, respectively, before calcination, decreased to only 7.0 and 7.7% respectively, after heat treatment. Furthermore, the noticeably different O/Sn ratios of the two films before annealing (i.e., 1.29 and 1.52 for the high and low duty cycles, respectively), became similar after thermal treatment (2.20 and 2.25). In fact, the overall atomic concentrations of Sn, O, and C were essentially similar after the annealing process. The atomic concentrations of each element depending on the treatment are summarized in Table 1. Additionally, it is also important to note that the nonconductive, electrically insulating as-deposited films became electrically conductive as a result of the heat treatment. This transformation became apparent during XPS analysis, in that the samples subjected to the annealing process no longer required neutralization to obtain accurate values of the photoelectron binding energies. Additionally, thermally annealed samples deposited on the flat glass plates exhibited sheet conductivity of the order of $\sim 10^{-4}$ $S \cdot cm^{-1}$, as measured using the standard four probe method. This value is of the order expected for a tin oxide film in which not all the tin is present as SnO_2.

XPS Characterization of F-Doped Tin Oxide Films. Because it has been reported that fluorine doping of SnO_2 increases its electrical conductivity, experiments were carried out to determine if the plasma surface modification process might be extended to production of F-doped tin oxide. In these experiments, a mixture (1:4 volume ratio) of TMT and perfluoropropylene oxide (C_3F_6O) were employed during the plasma polymerization step. Prior work from our laboratory has examined the pulsed plasma deposition of the perfluorocarbon monomer in some detail.[29] The TMT + C_3F_6O plasma depositions were carried out at a plasma on/off ratio of 10/50 (ms) and a peak power input of 150 W. High-resolution spectra of "as-deposited" and annealed (TMT + C_3F_6O) films were obtained, with the heat treatment again carried out at 425 °C. A summary of the XPS spectra for C, O, and F atoms is presented in Figure 6, reading from the top to the bottom. In this figure, spectra labeled a, c, and e are from the as-deposited films, whereas b, d, and f are the

(24) Sergent, N.; Gelin, P.; Perier-Camby, L.; Praliaud, H.; Thomas, G. *Phys. Chem. Chem. Phys.* **2002**, *4*, 4802.
(25) Hadjiivanov, K.; Reddy, B. M.; Knozinger, H. *Appl. Catal., A* **1999**, *188*, 355.
(26) Hadjiivanov, K.; Lamotte, J.; Lavalley, J. C. *Langmuir* **1997**, *13*, 3374
(27) Concepcion, P.; Reddy, B. M.; Knozinger, H. *Phys. Chem. Chem. Phys.* **1999**, *1*, 3031.
(28) Busca, G. *Catal. Today* **1998**, *41*, 191.
(29) Chen, X. Molecular tailoring of surfaces via pulsed RF plasma deposition. Ph.D. Dissertation, University of Texas at Arlington, Arlington, TX, 1995.

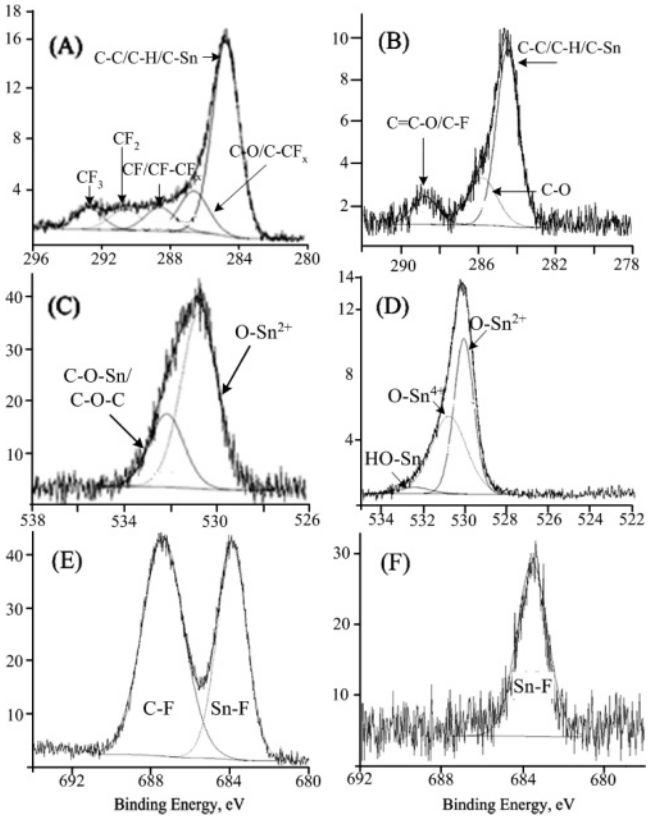

Figure 6. High-resolution C(1s), O(1s), and F(1s) (top to bottom) XPS spectra of films "as-deposited" and after heat treatment. Panels A, C, and E are the as-deposited films while B, D, and F are the heat-treated samples.

corresponding results after annealing. Whereas the as-deposited C(1s) spectrum contains both fluorocarbon (peaks at 288.5 and 290.5 eV) and hydrocarbon peaks (284.6 eV), the annealed sample exhibits a sharply reduced fluorocarbon content. The as-deposited high-resolution O(1s) spectrum consists of two broad components, assigned primarily to 530.3 eV ($O-Sn^{2+}$) and 531.9 eV ($C-O-Sn/C-O-C$), while the F(1s) photoelectrons reveal comparable amounts of fluorocarbons (687.4 eV) and tin fluoride (684 eV). The heat-treated samples clearly reveal the loss of carbon content with the O(1s) spectrum revealing only tin−oxygen bonds while the fluorine spectrum consists uniquely of Sn−F bonds. Thus, XPS results demonstrate that fluorine atoms are successfully incorporated into the tin-containing plasma polymer matrix by addition of C_3F_6O during TMT plasma polymerization, with the residual fluorine directly bonded to tin atoms after the heat treatment. These results reveal that it is indeed possible to dope the tin oxide with fluorine using this plasma deposition technique. It should be noted that high-resolution XPS spectra of the Sn content in these films were also carried out, but the relative insensitivity of the Sn binding energies in Sn−O, compared to Sn−F bonding, prevent direct observation of Sn−F bonds.[30] As in the work with the TMT monomer, it was observed that these fluorine doped films were clearly electrically conductive, as revealed during the recording of the XPS spectra.

(30) Cho, J. RF pulsed plasma surface modification of titanium dioxide nanoparticles for environmental applications. Ph.D. Dissertation, University of Texas at Arlington, Arlington, TX, 2005.

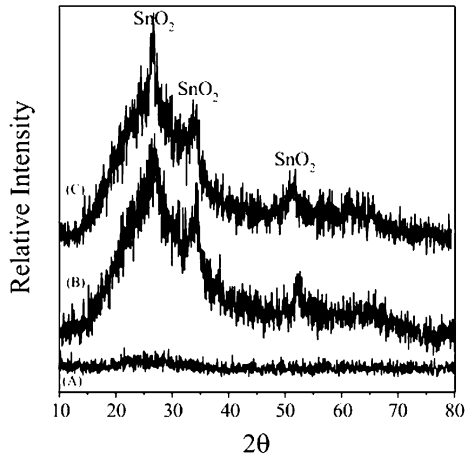

Figure 7. XRD spectra of RF pulsed plasma deposited films on glass slides with 10-ms-on/50-ms-off at 150 W. (A) The as-deposited film forms the TMT + C_3F_6O mixture. (B) The TMT only film after heat treatment at 425 °C. (C) The TMT + C_3F_6O film after heat treatment at 300 °C.

XRD Analyses. XRD studies were carried out to determine if a crystalline semiconducting SnO_2 phase was produced by annealing plasma films obtained from TMT plasma polymerizations. For this purpose the TMT only and TMT + C_3F_6O films were deposited on glass substrates because the presence of TiO_2 crystals exhibits scattering angles very similar to those of SnO_2 and would thus interfere with these measurements. The as-deposited plasma films obtained from both TMT-only and the TMT-C_3F_6O mixture plasma were observed to be amorphous, as illustrated in the bottom trace of Figure 7A for the TMT + C_3F_6O sample. However, after the heat treatment, clear evidence for SnO_2 crystal formation is revealed by diffraction peaks at 2θ angles of 26, 34, and 38, as shown in Figure 7B for TMT only and Figure 7C for TMT + C_3F_6O. The XRD patterns shown are for samples that exhibited the highest catalytic activities, namely, the TMT annealed at 425 °C and the TMT + C_3F_6O annealed at 300 °C. The crystallization of TMT-containing plasma films observed by XRD analyses are in agreement with the aforementioned XPS results which revealed the presence of tin oxides after annealing.

Morphology of TMT-Based Plasma Polymerized Films. Additional strong confirmatory evidence of the compositional changes of the films as a result of the heat treatments is provided by atomic force microscopic (AFM) examination of the films before and after annealing. These AFM measurements were carried out on films obtained from both pure TMT and the TMT + C_3F_6O mixture. In both cases the films were deposited on highly polished Si plates. The AFM results are presented in Figure 8. Panels A and C are scans obtained from the as-deposited films from pure TMT and the TMT + C_3F_6O mixture, respectively. The corresponding scans obtained after the heat treatment are shown in panels B and D. It is clear, for both samples, that the heat treatment produced a large increase in average surface roughness. Superimposed on the generally roughened surfaces are prominent sharp peaks. It is assumed that these peaks indicate the presence of crystallites on the surfaces produced by the high-temperature exposure. The density and size of these crystallites are somewhat more pronounced in the TMT + C_3F_6O than in the film obtained from pure TMT.

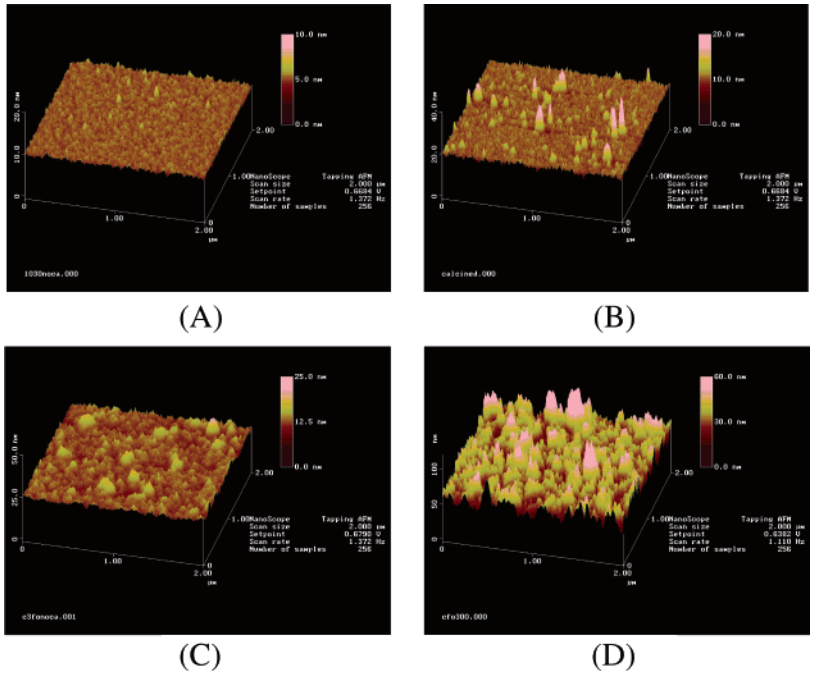

Figure 8. AFM image of (A) as-deposited and (B) heat-treated TMT only films; (C) as-deposited and (D) heat-treated TMT + C_3F_6O films.

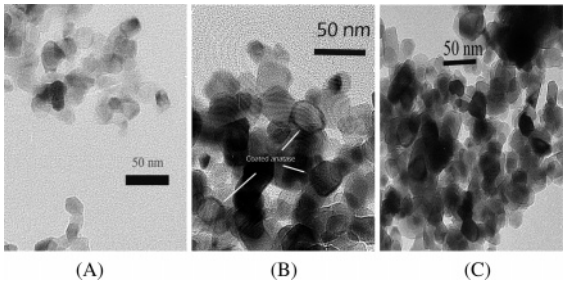

Figure 9. TEM bright field image of untreated and plasma coated TiO_2 nanoparticles before and after annealing at 450 °C for 5 h. (A) Untreated P-25 (340 000×); (B) TMT + C_3F_6O plasma coated TiO_2 before annealing (400 000×); and (C) TMT + C_3F_6O plasma coated TiO_2 after annealing (300 000×).

These AFM data are in accord of expectations based on the XPS and XRD studies of these same films.

In addition to the AFM studies on the plasma film on flat substrates, TEM images of the TMT + C_3F_6O coated TiO_2 particles, before and after annealing, were also obtained to provide clear visual evidence of the hybrid catalyst. The bright field TEM images of the higher resolution are shown in Figure 9. The images of the untreated and plasma treated TiO_2, with and without annealing, are compared in these figures. The highest magnification picture obtainable (340 000×) suggests the presence of the thin polymer coating on specific TiO_2 nanoparticles as shown and noted explicitly in Figure 9B. The overall dark and light contrasts observed in this figure are consistent with the presence of the polymer coating having been applied in that the heavier Sn atoms should appear darker than the TiO_2 components. The film thickness (a few nanometers) indicated in Figure 9B is consistent with what would be expected based on the deposition times employed. These figures also confirm that the Sn-containing components remain after the heat treatment.

Evaluation of Photocatalytic Activities of Modified and Unmodified TiO_2. To test the potential utility of plasma processing as a route to surface modification of catalysts, the photocatalytic activity of the plasma modified TiO_2 particles was carefully measured and contrasted with that of the unmodified TiO_2 P-25 starting material. These measurements were made under oxidative conditions using the organic dye, AO7. Oxidation of this compound leads to bleaching of the orange color of the AO7 solution, and thus the oxidation rate is easily monitored spectroscopically. A large number of kinetic runs were carried out using TiO_2 particles which had been coated with TMT only as well as with TMT + C_3F_6O films. All of these kinetic measurements were made under exactly identical reaction conditions with respect to the amount of catalyst, AO7 concentration, and light intensity. Catalyst activity measurements were made for both as-deposited and heat-treated composite particles.

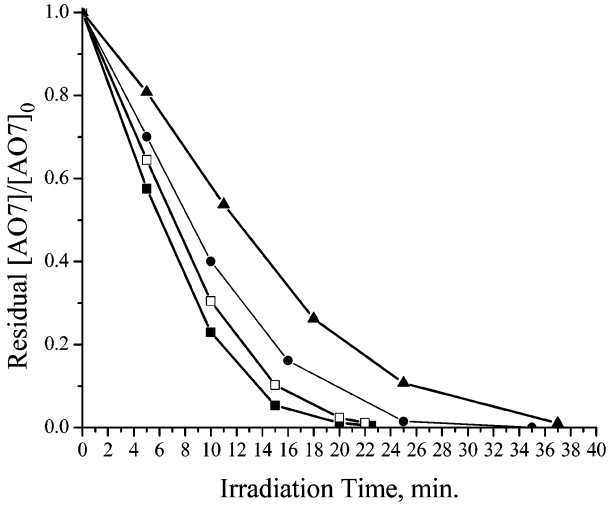

Figure 10. Relative photocatalytic oxidation rates of AO7 by unmodified TiO_2 and various TMT-based plasma hybrid TiO_2 particles. Each kinetic run involved 500 μM AO7 solution containing 300 mg of catalyst that was illuminated by 400 W UV light. ▲, As-deposited TMT + C_3F_6O; □, heat-treated TMT only; ■, heat-treated TMT + C_3F_6O; and ●, uncoated TiO_2 but calcined at 425 °C for 5 h.

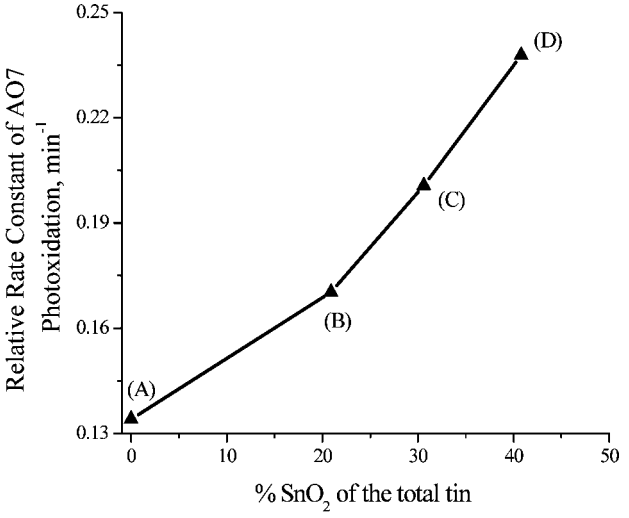

Figure 11. Plot of the relative first-order rate constants for oxidation of AO7 as a function of % SnO2 of the total tin present on each catalysts. (A) untreated TiO_2, (B) oxygen plasma and heat-treated sample obtained from a TMT only deposition, (C) heat-treated TMT only deposition, and (D) heat-treated TMT + C_3F_6O deposition.

Initial experiments revealed that heat treatment of the nonplasma treated TiO_2 improved its catalytic activity slightly, presumably by removal of some of the adsorbed carbonaceous material present on these particles. For that reason, the activity of the plasma treated particles was compared with that of heat-treated unmodified TiO_2. A number of general observations can be made concerning the catalytic activity of the plasma modified versus the unmodified TiO_2. One such generalization is that the TiO_2 with the "as-deposited" films, both the TMT only and the TMT + C_3F_6O mixture, were uniformly *less* active than the unmodified particles. In contrast, the heat-treated samples consistently exhibited a significantly *greater* catalytic activity than the untreated samples. Examples of these observations are shown in Figure 10, in which the oxidation rate of the AO7 is shown as a function of time for the as-deposited TMT + C_3F_6O material and both the heat-treated TMT only and the TMT + C_3F_6O samples. The oxidation rate for the calcined, but otherwise untreated, TiO_2 standard is also included in this figure for comparison. The decreased activity of the TiO_2 with the as-deposited films may arise from more than one source. One such source could be further oxidation of the plasma films at the expense of the AO7 molecules. Additionally this decrease could well arise from direct photon adsorption of short wavelength photons by the nonconductive polymer films, thus directly decreasing the rate of electron−hole generation.

The increased catalytic activity of the post-plasma heat-treated samples is attributed to the presence of conductive SnO_2 formed on the surface of the TiO_2 particles during the annealing process. The formation of the SnO_2 is documented directly by XPS and XRD and indirectly by AFM analyses as described above. In fact, because the XPS data provide a measure of the ratio of SnO_2/SnO present in the film, using those data and the AO7 oxidation rates, it is possible to quantify the importance of the conductive SnO_2 in improving TiO_2 activity. The AO7 photo-oxidation rates employed were obtained from a pseudo-first-order kinetic analysis of the degradation of AO7 as a function of irradiation time. The specific rate constants are equated to the slope of each first-order plot. The relative rate constants obtained from the identical photocatalytic reaction experiments are plotted in Figure 11 as a function of the SnO_2/SnO ratio for a series of samples containing essentially the same total tin content. It is clear that a strong correlation exists between the extent of surface SnO_2 and photocatalytic activity, with activity increasing with the relative content of SnO_2. The increased activity is significant in that the F doped TMT coating, annealed at 300 °C, exhibits an activity which is approximately 80% higher than that of the untreated TiO_2.

Discussion

The major focus of this study was to evaluate the utility of employing plasma processing as a route to functionalization of nanosized particles. It is well-known that the increased surface-to-volume ratios with decreasing particle size lead to increasing particle aggregation. This aggregation is sufficiently large to render ineffective typical conventional wet based coating technologies to modify surfaces of nanoparticles for specific applications. However, the availability of a 360° rotatable reactor, operable under PECVD conditions, offers an opportunity to provide vigorous agitation and mixing of nanoparticles during the coating process. In addition, it should be noted that the negative potential bias, acquired spontaneously by substrates in a plasma discharge, provide repulsive electrostatic interactions which presumably provide additional help to minimize particle aggregation. If this latter factor is effective, it would become increasingly important as the particle size decreases.

In the present work, selection of TiO_2 for evaluation of the PECVD coating technology was based on a number of considerations. One aspect centered on the fact that well-characterized nanoparticles are readily available (i.e., Degussa P-25), coupled with the knowledge that established catalytic reactions are available to test the overall efficacy of the coating procedure. Additionally, there is presently considerable interest in improving the photocatalytic activity of TiO_2 with respect to its usage in a wide variety of commercial applications, thus providing a more practical motivation for this selection. The choice of TMT as the monomer for this purpose was based on the fact that SnO_2 has been shown to be effective in promoting increased photocatalytic activity of TiO_2, coupled with the fact that we have had prior direct experience in PECVD studies of this compound.

As detailed above, it is clear that significantly increased photocatalytic activity was achieved using the PECVD approach. The basic mechanism involved in achieving increased activity by coupling selected other semiconductors with TiO_2 has been discussed and illustrated, in detail, in other reports.[1,12] In short, it is believed that the presence of a slight energy mismatch between the two semiconductors helps minimize electron−hole recombination processes. An important consideration in realizing this increased activity is to achieve good physical contact between the two semiconductors. We believe this is certainly true in the case of the plasma modified surfaces in that the original Sn-

containing plasma generated polymer is strongly grafted to the TiO_2 substrates under the high energy conditions prevailing during the plasma on periods. Furthermore, the subsequent high-temperature treatment to produce the tin oxide, while removing the carbon moieties, would promote even better contact with the TiO_2. The direct contact between the two semiconductors in the present work can be contrasted with that in other reports of composite materials produced by various physical mixing methods. Also significant, as shown in this work, the PECVD process can be adapted to achieve direct doping of the semiconductor coating applied to the core particle.

Finally, it should be noted that finer tuning of the current process in terms of the plasma parameters and deposition times should lead to composite particles of even greater photocatalytic activity than reported in the present paper. In particular, additional experiments involving variation in the extent of fluorine doping are of interest as would be work with various catalysts and other materials to gauge the general effectiveness of the PECVD approach in modifying the surfaces of nanoparticle substrates.

CM060212G